Journal of Power Sources 209 (2012) 130–140

Contents lists available at SciVerse ScienceDirect

Journal of Power Sources

journal homepage: www.elsevier.com/locate/jpowsour

Fractal-based theoretical model on saturation and relative permeability in the gas diffusion layer of polymer electrolyte membrane fuel cells

Ying Shi*, Shu Cheng, Shuhai Quan

School of Automation, Wuhan University of Technology, Hubei 430070, China

ARTICLE INFO

Article history:
Received 16 December 2011
Received in revised form 22 February 2012
Accepted 23 February 2012
Available online 3 March 2012

Keywords:
Diffusion medium
Saturation
Relative permeability
Hydrophobic
Hydrophilic
Fractal

ABSTRACT

After polytetrafluoroethylene (PTFE) treatment, due to the coexistence of hydrophilic and hydrophobic pores, the gas diffusion layer (GDL) of a polymer electrolyte membrane fuel cell (PEMFC) shows a character of mixed wettability, which in turn affects liquid water and mass transfer. A series of fractal models are developed in this work to investigate the effect of GDL's wettability on liquid water and gas permeation in GDL. Compared to the widely-used empirical models, the proposed model of saturation versus capillary pressure in a good agreement with experimental data is more suitable for the GDL of mixed wettability. By using this model, liquid water saturation is found to be positively correlated with tortuosity and pore area fractal dimensions for a hydrophilic case and hydrophilic pore fraction, whereas to be negatively correlated with these fractal dimensions for a hydrophobic case. Furthermore, theoretical predictions on gas and water relative permeability are made via the proposed models. Water relative permeability increases with the increases in the fractal dimensions for a hydrophobic GDL and liquid water saturation, whereas it decreases with the increases in the fractal dimensions for a hydrophilic GDL and hydrophilic pore fraction. For gas phase, an opposite result is obtained.

1. Introduction

Gas diffusion layer (GDL) is a component crucial for the operation of polymer electrolyte membrane fuel cell (PEMFC), as it plays an important role in the delivery of reactants from flow channels to catalyst layers and the effective removal of product water from the electrode. At higher current densities, a dramatic increase in reaction rates leads to the corresponding increase in water generation. Liquid water may fill the pore network within GDL and decrease the effective diffusivity of reactants through the layer. In the actual application of PEMFC, to facilitate the removal of liquid water, the GDL is usually treated with a non-wetting polymer such as polytetrafluoroethylene (PTFE) to create hydrophobic surfaces and pores throughout GDL, resulting in coexistence of the hydrophilic and hydrophobic pores and change in the wettability of diffusion medium.

The presence of excessive liquid water in the porous GDL blocks part of pores towards the catalyst, debilitating the performance of device. Pore scale phenomena associated with the presence of liquid water inside porous media and the effects of liquid water on capillary pressure, relative permeability of the wetting and non-wetting phases have become increasingly recognized in the recent years. Many experimental measurements and theoretical analysis have been taken to investigate the properties of porous GDL in the PEMFC.

Some of the experiments have been carried out to study the morphologic properties of the GDL by using mercury intrusion porosimetry (MIP) [1–6], which cannot distinguish between the hydrophilic and hydrophobic components of the diffusion medium. And most of these studies have focused on the dependence of capillary pressure on saturation for mercury–air system, while few have been concerned with that for water–air–GDL system, as required in mass transfer model. Gostick et al. [7] measured this dependence by using standard porosimetry method with water–air as working fluid pairs. Their following work [8] exploited an apparatus to survey the relationship between the air–water capillary pressure and water saturation, which enables the determination of the hydrophilic pore size distribution. Experimental measurements contribute a lot towards understanding the capillary behavior of water–air–GDL system, and always go with polynomial fits or empirical formulae.

For the GDLs, some researchers used a function that they developed from fitting data to relate the capillary pressure to the saturation [9,10,2], others adopted the van Genuchten model and the Brooks–Corey model [7], while majority described the relationship with the widely used and empirically determined Leverett J-function and its modified formulae [11–16], whose validity for their use in PEMFC modeling has recently received strong critics since they ignore the detail pore morphology of the GDL. In summary, there is much debate on the empirical expression between

* Corresponding author. Tel.: +86 18672952831; fax: +86 027 87859589.
E-mail address: a_laly@163.com (Y. Shi).

0378-7753/$ – see front matter © 2012 Elsevier B.V. All rights reserved.
doi:10.1016/j.jpowsour.2012.02.092

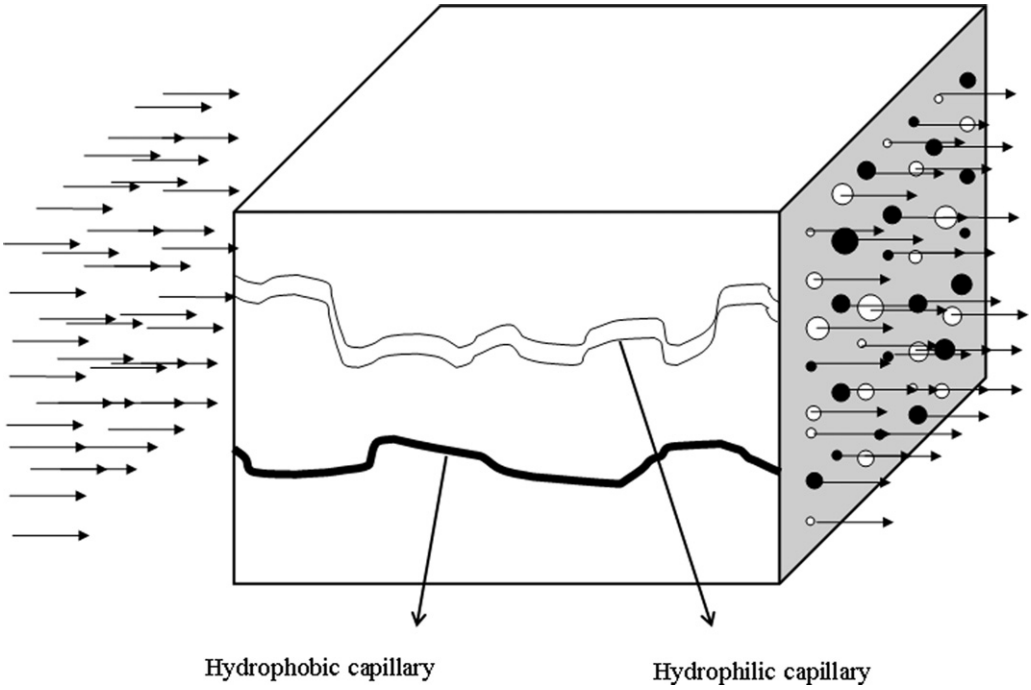

Fig. 1. Fractal bundle-of-hydrophilic-and-hydrophobic-capillaries model for porous GDL.

the capillary pressure and the saturation. Zamel and Li [17] and Wu et al. [18] compared several expressions to find out their effects on capillary pressure, and their research also showed that the choice of the empirical expression for capillary pressure is crucial for the simulation on liquid water transport in the PEMFC.

In general, the relation between capillary pressure and water saturation is used in numerical simulation for the theoretical research on the spatial distribution of liquid water and saturation in the GDLs. Wang and Nguyen [19], Zamel et al. [20] and Sinha and Wang [21] investigated the effect of capillary properties of the GDL on the liquid water transport and water saturation level using the numerical models. Most of the theoretical analyses employ the empirical expressions, although a short-coming is that their coefficients do not have a direct correlation to physical quantities, hindering the fundamental understanding of water percolation and movement within the diffusion medium.

Except for the above-mentioned drawback, the models for theoretical analysis mostly treat the GDL as entirely hydrophilic, which means that the liquid pressure must always be below the gas pressure. It is taken into account in the models by assuming the saturation with a value of zero at the interface of a diffusion medium with a gas channel, corresponding to the liquid pressure much lower than the gas pressure (and even approaching a value of zero) at this interface [22]. Since the GDLs have added PTFE to keep them from flooding, the coexistence of hydrophilicity and hydrophobicity of GDL results in a mixed-wetting characteristic, which was experimentally confirmed by Gostick et al. [7], the assumption of entirely hydrophilicity seems not to be valid.

The mixed wettability characteristics are caused by the wide range of wetting characteristics of carbon-based materials typically used for the PEMFC GDL, possible anomaly in the PTFE treatment and surface defects, impurities and aging of the GDL [21]. Only few researchers have considered the GDL as partially hydrophobic. Weber et al. [23] proposed a composite contact angle as a function of the fraction of hydrophilic pores in order to take the mixed wettability of GDL into account, and showed that there is an optimum fraction value of hydrophilic pores for approaching maximum limiting current and power. Nava et al. [12] determined the saturation by averaging the values for both the hydrophobic and hydrophilic pores according to the hydrophilic pore fraction and calculated the capillary pressure on the dependence of the saturation value with respect to this fraction. He et al. [24] discussed the saturations for the hydrophilicity and hydrophobicity case respectively and also averaged their values according to the hydrophilic pore fraction. Weber [25] integrated analytically the separate hydrophobic and hydrophilic pore-size distributions of the diffusion medium via a random cut-and-rejoin bundle-of-capillaries model, and combined their values to get the saturation according to the value range of contact angle.

On the view of theoretical research, the integral representation method is mathematically more constitutive than others because it conforms to the pattern of liquid water movement through the hydrophilic and hydrophobic pores rather than simply synthesizes according to the hydrophilic pore fraction. For this integral method, it is crucial to determine the pore-size distribution. Weber [25] assumed a series of log-normal distributions to fit the pore size distribution. Our previous study [26] experimentally provided insight about the fractal characteristic of the GDL in PEMFC, and the fractal pore size distribution can be used in the integral method.

The objective of the present work is to determine the dependence of the capillary pressure on the saturation and the relative permeability of gas and liquid water by a fractal bundle-of-hydrophilic-and-hydrophobic-capillaries model. And the paper is organized as follows: first, a fractal pore-network model for a mixed-wetting carbon paper GDL is described. Then, the expression between the capillary pressure and the saturation and the relative permeability models of gas and liquid water are presented. At last, the parametric effect analysis is taken.

2. Fractal porous-medium model for the GDL

Experimental investigations on permeation in porous media have shown that the channels through which liquids permeate have fractal characteristics. Similarly, the gas transfer routes within porous media may also have fractal characteristics and can be represented as random fractal curves. In PEMFC, porous carbon paper,

made from graphite fibers and used for the preparation of diffusion medium, GDL, shows a fractal characteristic. The gas and water permeation within the GDL can be assumed to be similar to that within the tortuous fractal parallel channels with different hydrophilic and hydrophobic pore sizes, depicted in Fig. 1.

The length $L(\lambda)$ of the capillary pathway is related to the capillary size λ (i.e., the pore diameter) by the following fractal relationship [27]

$$\frac{L(\lambda)}{L_0} = \left(\frac{L_0}{\lambda}\right)^{D_t-1} \tag{1}$$

where L_0 is the representative or linear length of these capillary pathways towards the flowing direction, and D_t is the tortuousity fractal dimension. Then $L(\lambda)$ is

$$L(\lambda) = {L_0}^{D_t}\lambda^{1-D_t} \tag{2}$$

And the tortuosity of the capillary pathway τ can be described by

$$\tau = \left(\frac{L(\lambda)}{L_0}\right)^2 = \left(\frac{L_0}{\lambda}\right)^{2D_t-2} \tag{3}$$

Another characteristic of porous media is that the cumulative pore population N in a unit cross section may be mathematically expressed as follows [27]:

$$N(d \geq \lambda) = \left(\frac{\lambda_{max}}{\lambda}\right)^{D_p} \tag{4}$$

where D_p is the pore area fractal dimension, and λ, λ_{max} are the pore size and the maximum pore size of porous media, respectively. The first derivative of Eq. (10) with respect to λ is

$$-dN = D_p\lambda_{max}^{D_p}\lambda^{-(D_p+1)}d\lambda \tag{5}$$

As mentioned above, the porous diffusion medium, GDL, can be considered as a composite structure with hydrophilic (usually carbon) and hydrophobic (usually Teflon) capillaries, and the number of former with diameter greater than λ is determined by [28]

$$N_{hi}(d \geq \lambda) = f_{hi}\left(\frac{\lambda_{max}}{\lambda}\right)^{D_p} \tag{6}$$

where f_{hi} is the fraction of hydrophilic pores, which is determined by the PTFE loading.

The proposed fractal bundle-of-hydrophilic-and-hydrophobic-capillaries model will be used to characterize a real carbon paper. Although this model is not correct on the local, pore-scale level, it is believed that it remains valid at the macroscopic, layer-scale level for its enough description on the real carbon paper. All the following derivations are based on this model.

3. Capillary pressure-liquid phase saturation relationships for diffusion medium

Under the dry condition, the hydrophilicity or hydrophobicity of GDL has no effect on the gas transport, but under the wet condition, the gas transport within GDL is highly related to water transport, which is in turn influenced by the mixed wettability of GDL.

The wettability of the GDL is related to capillary-driven liquid water behavior, described by the Young–Laplace equation

$$\lambda_c = -\frac{4\gamma\ \cos\theta}{p_c} \tag{7}$$

where λ_c is the pore diameter, γ is the surface tension of water, θ is the composite contact angle of water on the solid surface of the pore wall, and p_c is the capillary pressure, calculated by [23]

$$p_c = p_L - p_G \tag{8}$$

where p_L and p_G represent the liquid water and gas pressure, respectively. Usually the gas pressure can be considered as a constant in the fuel cell [29], so the capillary pressure becomes a direct relation of the liquid water pressure.

For hydrophilic case, the value of λ_c is the largest water-filled pore diameter, and the contact angle is $0^\circ \leq \theta < 90^\circ$. As for hydrophobic case, λ_c is the smallest water-filled pore diameter, and $90^\circ < \theta \leq 180^\circ$.

Existence of both hydrophilic and hydrophobic capillaries makes it difficult to investigate the wettability of GDL. The liquid saturation of diffusion medium is used for describing the mixed wettability, and is defined as the fraction of void space filled by liquid water phase

$$s = \frac{v_{water}}{v_{pores}} \tag{9}$$

where v_{water} is the volume of capillaries or pores filled with water, and v_{pores} is the total volume of the tortuous capillaries or pores.

If $p_c < 0$, i.e., at a negative capillary pressure, only the hydrophilic capillaries with diameter less than the critical diameter λ_{hi}^* are occupied by liquid water, then the liquid saturation s is

$$\begin{aligned} s &= \frac{-\int_{\lambda_{min}}^{\lambda_{hi}^*}(\pi/4)\lambda^2 L(\lambda)dN_{hi}}{-\int_{\lambda_{min}}^{\lambda_{max}}(\pi/4)\lambda^2 L(\lambda)dN} \\ &= f_{hi}\frac{(\lambda_{hi}^*)^{3-D_t-D_p} - \lambda_{min}^{3-D_t-D_p}}{\lambda_{max}^{3-D_t-D_p} - \lambda_{min}^{3-D_t-D_p}} \end{aligned} \tag{10}$$

where λ_{min} is the minimum pore size of porous media.

If $p_c = 0$, i.e., at a zero capillary pressure, all the hydrophilic capillaries are filled and all the hydrophobic capillaries are empty, and the liquid saturation s is

$$s = \frac{-\int_{\lambda_{min}}^{\lambda_{max}}(\pi/4)\lambda^2 L(\lambda)dN_{hi}}{-\int_{\lambda_{min}}^{\lambda_{max}}(\pi/4)\lambda^2 L(\lambda)dN} = f_{hi} \tag{11}$$

If $p_c > 0$, i.e., at a positive capillary pressure, all the hydrophilic capillaries and the hydrophobic capillaries with diameter greater than the critical diameter λ_{ho}^* are occupied, and the liquid saturation s is

$$\begin{aligned} s &= \frac{-\int_{\lambda_{min}}^{\lambda_{max}}(\pi/4)\lambda^2 L(\lambda)dN_{hi} - \int_{\lambda_{ho}^*}^{\lambda_{max}}(\pi/4)\lambda^2 L(\lambda)d(N-N_{hi})}{-\int_{\lambda_{min}}^{\lambda_{max}}(\pi/4)\lambda^2 L(\lambda)dN} \\ &= \frac{\lambda_{max}^{3-D_t-D_p} - f_{hi}\lambda_{min}^{3-D_t-D_p} - (1-f_{hi})(\lambda_{ho}^*)^{3-D_t-D_p}}{\lambda_{max}^{3-D_t-D_p} - \lambda_{min}^{3-D_t-D_p}} \\ &= 1-(1-f_{hi})\frac{(\lambda_{ho}^*)^{3-D_t-D_p} - \lambda_{min}^{3-D_t-D_p}}{\lambda_{max}^{3-D_t-D_p} - \lambda_{min}^{3-D_t-D_p}} \end{aligned} \tag{12}$$

From Eqs. (10)–(12), it is easy to know that the capillaries in the GDL are occupied by more and more liquid water with the increase of the capillary pressure or the liquid water pressure, according to the following order as: first the small hydrophilic capillaries, then the large hydrophilic capillaries followed by the large hydrophobic capillaries, and last the small hydrophobic capillaries.

According to Eqs. (10)–(12), the liquid saturation of the GDL can be described with a piecewise function

$$s=\begin{cases} f_{\mathrm{hi}}\dfrac{(\lambda_{\mathrm{hi}}^{*})^{3-D_t-D_p}-\lambda_{\min}^{3-D_t-D_p}}{\lambda_{\max}^{3-D_t-D_p}-\lambda_{\min}^{3-D_t-D_p}} & p_c<0\\ f_{\mathrm{hi}} & p_c=0\\ 1-(1-f_{\mathrm{hi}})\dfrac{(\lambda_{\mathrm{ho}}^{*})^{3-D_t-D_p}-\lambda_{\min}^{3-D_t-D_p}}{\lambda_{\max}^{3-D_t-D_p}-\lambda_{\min}^{3-D_t-D_p}} & p_c>0 \end{cases} \tag{13}$$

And then the relation between the capillary pressure and the liquid saturation can be obtained by substituting Eq. (7) into Eq. (13)

$$s=\begin{cases} f_{\mathrm{hi}}\dfrac{(-((4\gamma\cos\theta_{\mathrm{hi}})/p_c))^{3-D_t-D_p}-\lambda_{\min}^{3-D_t-D_p}}{\lambda_{\max}^{3-D_t-D_p}-\lambda_{\min}^{3-D_t-D_p}} & p_c<0\\ f_{\mathrm{hi}} & p_c=0\\ 1-(1-f_{\mathrm{hi}})\dfrac{(-((4\gamma\cos\theta_{\mathrm{ho}})/p_c))^{3-D_t-D_p}-\lambda_{\min}^{3-D_t-D_p}}{\lambda_{\max}^{3-D_t-D_p}-\lambda_{\min}^{3-D_t-D_p}} & p_c>0 \end{cases} \tag{14}$$

where θ_{hi} is the contact angle for the hydrophilic phase and θ_{ho} is the contact angle for the hydrophobic coating.

From Eqs. (13) and (14), it can be seen that the liquid saturation of the diffusion medium is a continuous function of the capillary pressure, and if $p_c<0$, since $\lambda_{\mathrm{hi}}^{*}<\lambda_{\max}$, then $s<f_{\mathrm{hi}}$; if $p_c>0$, because $\lambda_{\mathrm{ho}}^{*}<\lambda_{\max}$, $s>f_{\mathrm{hi}}$, and Eq. (14) can also be rewritten as

$$s=\begin{cases} f_{\mathrm{hi}}\dfrac{(-(4\gamma\cos\theta_{\mathrm{hi}}/p_c))^{3-D_t-D_p}-\lambda_{\min}^{3-D_t-D_p}}{\lambda_{\max}^{3-D_t-D_p}-\lambda_{\min}^{3-D_t-D_p}} & s<f_{\mathrm{hi}}\\ 1-(1-f_{\mathrm{hi}})\dfrac{(-(4\gamma\cos\theta_{\mathrm{ho}}/p_c))^{3-D_t-D_p}-\lambda_{\min}^{3-D_t-D_p}}{\lambda_{\max}^{3-D_t-D_p}-\lambda_{\min}^{3-D_t-D_p}} & s>f_{\mathrm{hi}} \end{cases} \tag{15}$$

Because there is no liquid transport at the residual liquid saturation, s_r, an effective liquid saturation, s_e, which can be interpreted as the fraction of transportable liquid, has to be taken into account as follows:

$$s_e=\frac{s-s_r}{1-s_r} \tag{16}$$

4. Fractal model on relative permeability in diffusion medium

4.1. Fractal model on water relative permeability in diffusion medium

The water relative permeability is of great importance for species simulation in the GDL. The flow rate $q(\lambda)$ through a single tortuous capillary with a diameter, λ, is given by modifying the well known Hagen–Poiseulle equation [30]

$$q(\lambda)=\frac{\pi}{128}\frac{\Delta p}{L(\lambda)}\frac{\lambda^4}{\mu} \tag{17}$$

where ΔP is the pressure gradient, and μ is the viscosity of the fluid. Then the total volumetric flow rate Q can be obtained by integrating the individual flow rate $q(\lambda)$ over the entire range of pore sizes from the minimum pore size $\lambda_{\min}$ to the maximum pore size $\lambda_{\max}$ in a unit cell according to the fractal bundle-of-hydrophilic-and-hydrophobic-capillaries model, as follows:

$$Q=-\int_{\lambda_{\min}}^{\lambda_{\max}} q(\lambda)dN \tag{18}$$

According to the value range of capillary pressure, the total flow rate of water Q_w is

$$Q_w=\begin{cases} -\displaystyle\int_{\lambda_{\min}}^{\lambda_{\mathrm{hi}}^{*}} q(\lambda)dN_{\mathrm{hi}} & p_c<0\\ -\displaystyle\int_{\lambda_{\min}}^{\lambda_{\max}} q(\lambda)dN_{\mathrm{hi}} & p_c=0\\ -\displaystyle\int_{\lambda_{\min}}^{\lambda_{\max}} q(\lambda)dN_{\mathrm{hi}}-\int_{\lambda_{\mathrm{ho}}^{*}}^{\lambda_{\max}} q(\lambda)d(N-N_{\mathrm{hi}}) & p_c>0 \end{cases} \tag{19}$$

Using Darcy's law, we can obtain the permeability for saturated porous diffusion medium

$$K=\frac{\mu L_0 Q}{\Delta p A} \tag{20}$$

and the permeability for liquid water

$$K_w=\frac{\mu_w L_0 Q_w}{\Delta p_w A} \tag{21}$$

where μ_w is the viscosity of water, Δp_w is the pressure gradient of water, and A is the representative area.

Substituting Eqs. (2), (5), (17) and (18) into Eq. (20), we have

$$K=\frac{\pi}{128}\frac{L_0^{1-D_t}}{A}\frac{D_p\lambda_{\max}^{D_p}}{3-D_p+D_t}(\lambda_{\max}^{3-D_p+D_t}-\lambda_{\min}^{3-D_p+D_t}) \tag{22}$$

And according to Eqs. (2), (5), (6), (17), (19) and (21), we obtain

$$K_w=\begin{cases} \dfrac{\pi}{128}\dfrac{L_0^{1-D_t}}{A}\dfrac{f_{\mathrm{hi}}D_p\lambda_{\max}^{D_p}}{3-D_p+D_t}[(\lambda_{\mathrm{hi}}^{*})^{3-D_p+D_t}-\lambda_{\min}^{3-D_p+D_t}] & p_c<0\\ \dfrac{\pi}{128}\dfrac{L_0^{1-D_t}}{A}\dfrac{f_{\mathrm{hi}}D_p\lambda_{\max}^{D_p}}{3-D_p+D_t}(\lambda_{\max}^{3-D_p+D_t}-\lambda_{\min}^{3-D_p+D_t}) & p_c=0\\ \dfrac{\pi}{128}\dfrac{L_0^{1-D_t}}{A}\dfrac{D_p\lambda_{\max}^{D_p}}{3-D_p+D_t}[\lambda_{\max}^{3-D_p+D_t}-f_{\mathrm{hi}}\lambda_{\min}^{3-D_p+D_t} & \\ -(1-f_{\mathrm{hi}})(\lambda_{\mathrm{ho}}^{*})^{3-D_p+D_t}] & p_c>0 \end{cases} \tag{23}$$

Combining Eqs. (22), (23) and the definition of the water relative permeability yields

$$k_{rw}=\frac{K_w}{K}=\begin{cases} f_{\mathrm{hi}}\dfrac{(\lambda_{\mathrm{hi}}^{*})^{3-D_p+D_t}-\lambda_{\min}^{3-D_p+D_t}}{\lambda_{\max}^{3-D_p+D_t}-\lambda_{\min}^{3-D_p+D_t}} & p_c<0\\ f_{\mathrm{hi}} & p_c=0\\ f_{\mathrm{hi}}+\dfrac{(1-f_{\mathrm{hi}})[\lambda_{\max}^{3-D_p+D_t}-(\lambda_{\mathrm{ho}}^{*})^{3-D_p+D_t}]}{\lambda_{\max}^{3-D_p+D_t}-\lambda_{\min}^{3-D_p+D_t}} & p_c>0 \end{cases} \tag{24}$$

From Eq. (24), it can be seen that the water relative permeability is a continuous function of the capillary pressure, and if $p_c<0$, since $\lambda_{\mathrm{hi}}^{*}<\lambda_{\max}$, then $k_{rw}<f_{\mathrm{hi}}$; if $p_c>0$, because $\lambda_{\min}<\lambda_{\mathrm{ho}}^{*}<\lambda_{\max}$, $f_{\mathrm{hi}}<k_{rw}<1$, and Eq. (24) can be reduced as

$$k_{rw}=\begin{cases} f_{\mathrm{hi}}\dfrac{(\lambda_{\mathrm{hi}}^{*})^{3-D_p+D_t}-\lambda_{\min}^{3-D_p+D_t}}{\lambda_{\max}^{3-D_p+D_t}-\lambda_{\min}^{3-D_p+D_t}} & k_{rw}<f_{\mathrm{hi}}\\ f_{\mathrm{hi}}+\dfrac{(1-f_{\mathrm{hi}})\left[\lambda_{\max}^{3-D_p+D_t}-(\lambda_{\mathrm{ho}}^{*})^{3-D_p+D_t}\right]}{\lambda_{\max}^{3-D_p+D_t}-\lambda_{\min}^{3-D_p+D_t}} & k_{rw}>f_{\mathrm{hi}} \end{cases} \tag{25}$$

According to Eq. (25), the water relative permeability is also a continuous function of the hydrophilic pore fraction f_{hi}.

4.2. Fractal model on the relative permeability of gas in diffusion medium

In the simulation of PEMFC, the gas permeability diffusion in GDL also needs to be taken into account.

At a negative capillary pressure, only the hydrophilic capillaries with diameter less than the critical diameter $\lambda_{\mathrm{hi}}^{*}$ are occupied by

Table 1
Values for model parameters and physical properties of GDL material tested.

Parameter		Value
Hydrophilic pore fraction	f_{hi}	0.35
Contact angle for water on graphite [23]	θ_{hi}	80°
Contact angle for water on PTFE [23]	θ_{ho}	110°
Residual liquid saturation [25]	s_r	0.05
Water surface tension [23]	γ	$0.12398-0.00017393 \cdot T\ \mathrm{N\,m^{-1}}$
Maximum pore diameter [24]	λ_{max}	1.0661×10^{-4} m
Minimum pore diameter	λ_{min}	2.5×10^{-6} m
Pore area dimension [31]	D_p	1.9669
Tortuosity dimension [31]	D_t	1.1447
Operation temperature	T	333 K
Absolute permeability [31]	K	8×10^{-12} m^2
Porosity [31]	ε	0.78

liquid water, gas can pass through the rest capillaries, and then the total flow rate of gas Q_g is

$$Q_g = -\int_{\lambda_{min}}^{\lambda_{max}} q(\lambda)dN + \int_{\lambda_{min}}^{\lambda_{hi}^*} q(\lambda)dN_{hi} \tag{26}$$

At a zero capillary pressure, all the hydrophilic capillaries are filled with water, gas can pass through all the hydrophobic capillaries, and the total flow rate of gas Q_g is

$$Q_g = -\int_{\lambda_{min}}^{\lambda_{max}} q(\lambda)d(N - N_{hi}) \tag{27}$$

For a positive capillary pressure, all the hydrophilic capillaries and the hydrophobic capillaries with diameter greater than the critical diameter λ_{ho}^* are occupied by water and the total flow rate of gas Q_g is

$$Q_g = -\int_{\lambda_{min}}^{\lambda_{ho}^*} q(\lambda)d(N - N_{hi}) \tag{28}$$

Combining Eqs. (2), (5), (6), (26), (27) and (28), the gas permeability can be gained by

$$K_g = \begin{cases} \dfrac{\pi}{128}\dfrac{L_0^{1-D_t}}{A}\dfrac{D_p\lambda_{max}^{D_p}}{3-D_p+D_t}[\lambda_{max}^{3-D_p+D_t} & \\ \quad -f_{hi}(\lambda_{hi}^*)^{3-D_p+D_t} - (1-f_{hi})\lambda_{min}^{3-D_p+D_t}] & p_c < 0 \\ \dfrac{\pi}{128}\dfrac{L_0^{1-D_t}}{A}\dfrac{(1-f_{hi})D_p\lambda_{max}^{D_p}}{3-D_p+D_t}(\lambda_{max}^{3-D_p+D_t} - \lambda_{min}^{3-D_p+D_t}) & p_c = 0 \\ \dfrac{\pi}{128}\dfrac{L_0^{1-D_t}}{A}\dfrac{(1-f_{hi})D_p\lambda_{max}^{D_p}}{3-D_p+D_t}[(\lambda_{ho}^*)^{3-D_p+D_t} - \lambda_{min}^{3-D_p+D_t}] & p_c > 0 \end{cases} \tag{29}$$

And the relative permeability of gas is

$$k_{rg} = \frac{K_g}{K} = \begin{cases} 1 - f_{hi} + \dfrac{f_{hi}[\lambda_{max}^{3-D_p+D_t} - (\lambda_{hi}^*)^{3-D_p+D_t}]}{\lambda_{max}^{3-D_p+D_t} - \lambda_{min}^{3-D_p+D_t}} & p_c < 0 \\ 1 - f_{hi} & p_c = 0 \\ (1-f_{hi})\dfrac{(\lambda_{ho}^*)^{3-D_p+D_t} - \lambda_{min}^{3-D_p+D_t}}{\lambda_{max}^{3-D_p+D_t} - \lambda_{min}^{3-D_p+D_t}} & p_c > 0 \end{cases} \tag{30}$$

It can also be reduced as

$$k_{rg} = \begin{cases} 1 - f_{hi} + \dfrac{f_{hi}[\lambda_{max}^{3-D_p+D_t} - (\lambda_{hi}^*)^{3-D_p+D_t}]}{\lambda_{max}^{3-D_p+D_t} - \lambda_{min}^{3-D_p+D_t}} & k_{rg} > 1 - f_{hi} \\ (1-f_{hi})\dfrac{(\lambda_{ho}^*)^{3-D_p+D_t} - \lambda_{min}^{3-D_p+D_t}}{\lambda_{max}^{3-D_p+D_t} - \lambda_{min}^{3-D_p+D_t}} & k_{rg} < 1 - f_{hi} \end{cases} \tag{31}$$

5. Results and discussion

From the above-mentioned derivations, we can see that the p_c–s correlation is significant to the proposed models. As far as the p_c–s correlation is concerned, a mention should be made concerning hysteresis, which is common in the porous media literature. Several researchers [25,31,32] have observed the hysteretic wetting between liquid and gas intrusion into the GDL, which demonstrates preferential wetting of the pores, the importance of history, and that the GDL pores exhibit intermediate wettability [25]. It is largely due to "ink-bottle" effects and hysteresis in the contact angle [31]. Here we have derived the p_c–s correlation according to the process of liquid intrusion, without regard to that of gas intrusion.

Table 2
Fitting parameters for various empirical relations.

Parameter	Value
P_{cb1}	0.8040 kPa
P_{cb2}	0.7655 kPa
n	15.2839
m	0.0678
ν	1.0016

From the above fractal models of saturation (see Eqs. (14) and (15)) and relative permeability of water and gas (see Eqs. (24), (25), (30) and (31)), it can be seen that both the liquid water saturation and the relative permeability are determined not only by capillary pressure, contact angles and water surface tension but also by the GDL structure parameters (f_{hi}, λ_{max}, λ_{min}, D_p and D_t). For the following theoretical analysis, a set of parameters and operating conditions has been specified as the base case, which comes from the literatures [23–25,33], as listed in Table 1.

5.1. Predicted saturation

The saturation depends on the capillary pressure, which is a quantitative measure of the liquid water transport in the GDL and is related to the diffusive transport of liquid water since the liquid water diffusion coefficient is defined in terms of the capillary pressure [20]. Several models are commonly used to fit p_c–s curves. The most widely used one is the Leverett J-function model [20]

$$p_c = \gamma \cos\theta\left(\frac{\varepsilon}{K}\right)^{0.5} f(s) \tag{32}$$

where ε is the air-filled porosity, K is the absolute permeability, and the term $f(s)$, called the Leverett J-function, represents the dimensionless capillary pressure as a function of liquid saturation and is given as

$$f(s) = \begin{cases} 1.417(1-s) - 2.120(1-s)^2 + 1.263(1-s)^3 & \text{if } 0° \le \theta < 90° \\ 1.417s - 2.120s^2 + 1.263s^3 & \text{if } 90° \le \theta < 180° \end{cases} \tag{33}$$

Other common models are the van Genuchten model (Eq. (34)) and the Brooks–Corey model (Eq. (35)) [7].

$$s = \left(1 + \left(\frac{p_c}{p_{cb1}}\right)^n\right)^{-m}; \quad p_c > 0 \tag{34}$$

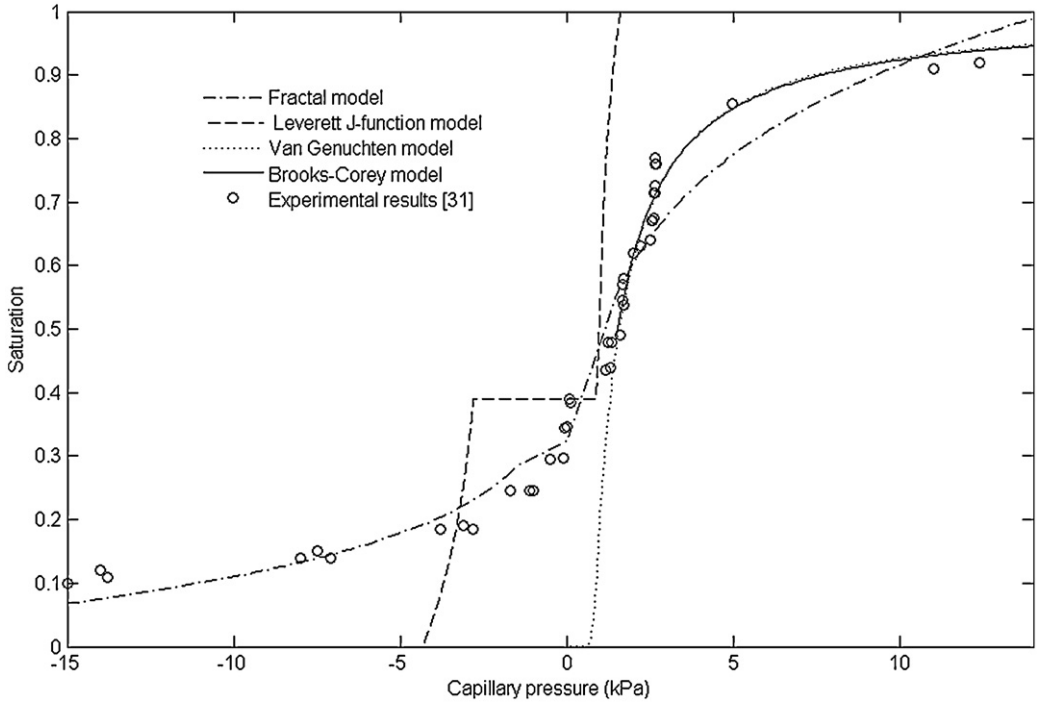

Fig. 2. Capillary pressures from the fractal and empirical models compared to experimental data of the study by Fairweather et al. [31].

$$s = \left(\frac{p_c}{p_{cb2}}\right)^{-\upsilon}; \quad p_c > p_{cb2} \tag{35}$$

where p_{cb1}, p_{cb2}, n, m, υ are fitting parameters.

The present fractal model is compared with the above empirical models and the experimental data complied from the literature [31], as shown in Fig. 2. These experimental data are obtained from the process of liquid intrusion, which corresponds with the assumption of our models. The fitting parameters of the van Genuchten model or the Brooks–Corey model can be determined from a best fit of the model to experimental data, as given in Table 2. The best fit is determined by the lowest root sum of squared error between the experimental data and the capillary model. And the value of hydrophilic pore fraction in the fractal model is assumed to 0.35 for the hydrophobic tendency of the experimental sample. As can be seen, the results of our fractal model are in better agreement with the experimental data than other empirical models. Hereinto, the Leverett J-function model overestimates the saturation, and the curve slope of this function is only close to that of experimental

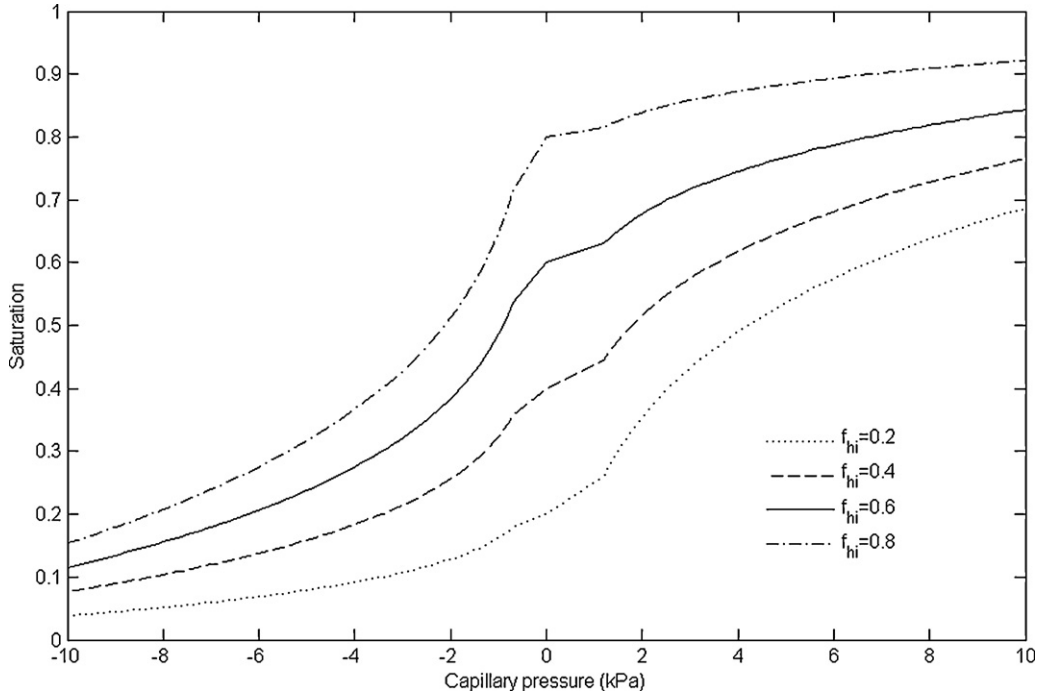

Fig. 3. Liquid water saturations as function of capillary pressure for different hydrophilic pore fraction.

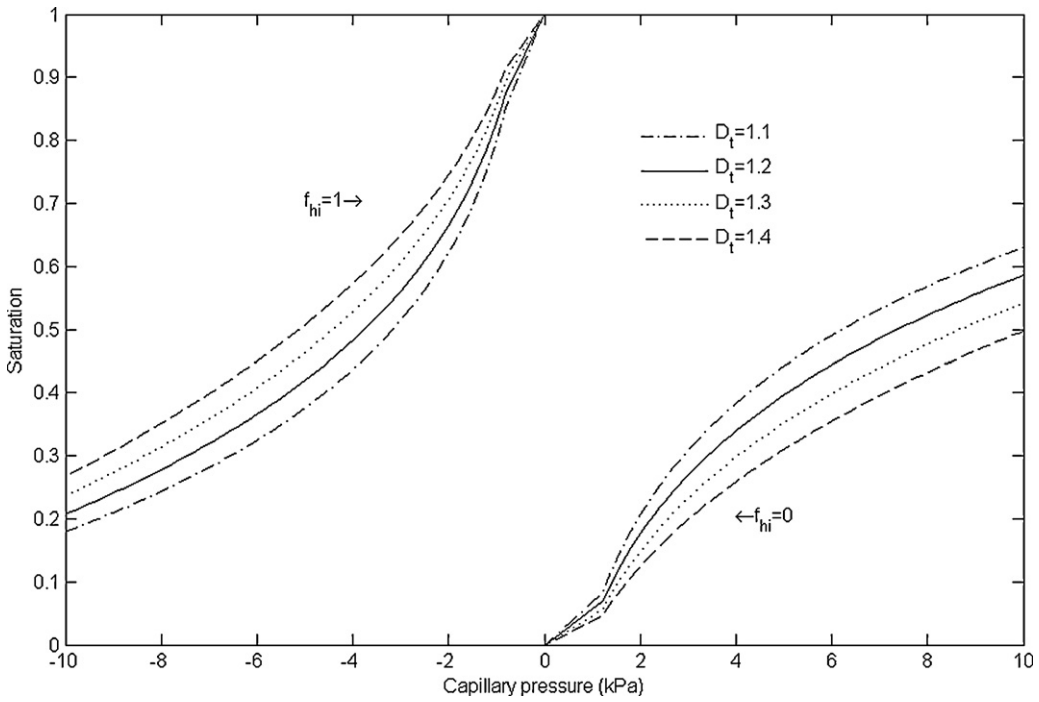

Fig. 4. Effect of tortuosity fractal dimension D_t on liquid water saturation.

data during a small range. As for the van Genuchten model and the Brooks–Corey model, data points below zero capillary pressure and p_{cb2} are excluded respectively, since these models cannot describe the behavior in these regions. Although these empirical models agree well with part of experimental data for the hydrophilic case, they show a bad consistent with the experimental data in the case of mixed wettability, depicted in Fig. 2. Furthermore, a drawback of all these empirical models is that they do not reveal any direct relationship between p_c–s curve and the GDL structure.

From Fig. 2, it also can be seen that the saturation varies slowly with negative capillary pressure while varies greatly with positive capillary pressure because the sample with a small hydrophilic pore fraction includes few hydrophilic-like pores corresponding to negative capillary pressure and many hydrophobic-like pores corresponding to positive capillary. Moreover, the saturation increases as capillary pressure increases from negative value to positive one.

In order to investigate the effect of PTFE on the p_c–s curve, different values of hydrophilic pore fraction were chosen, as illustrated in

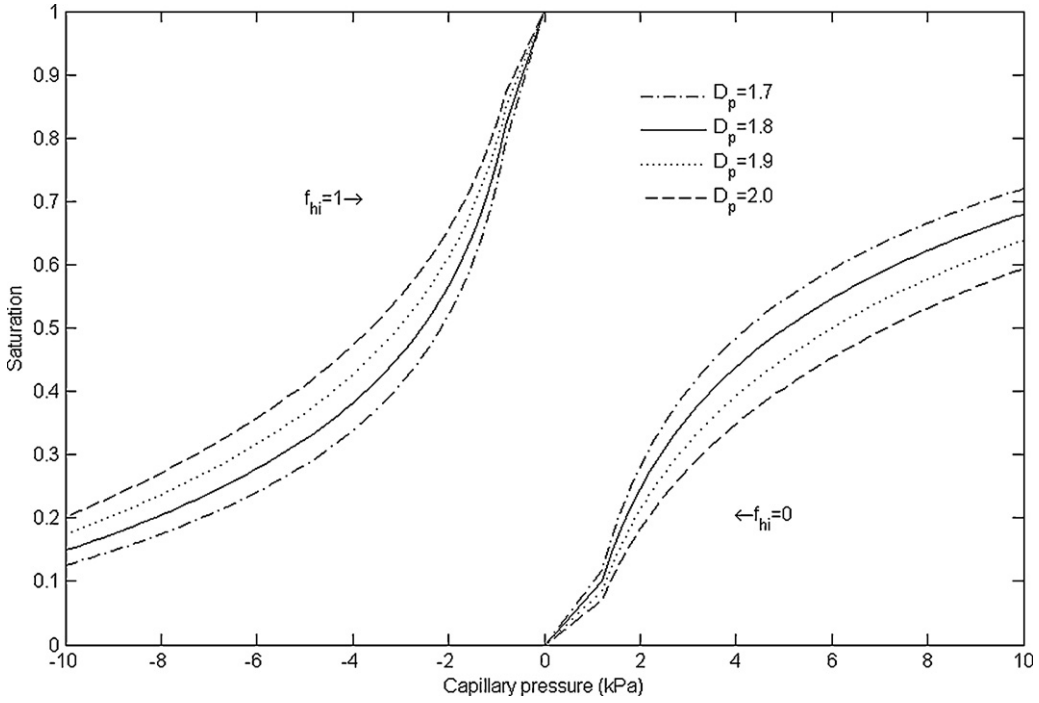

Fig. 5. Effect of pore area fractal dimension D_p on liquid water saturation.

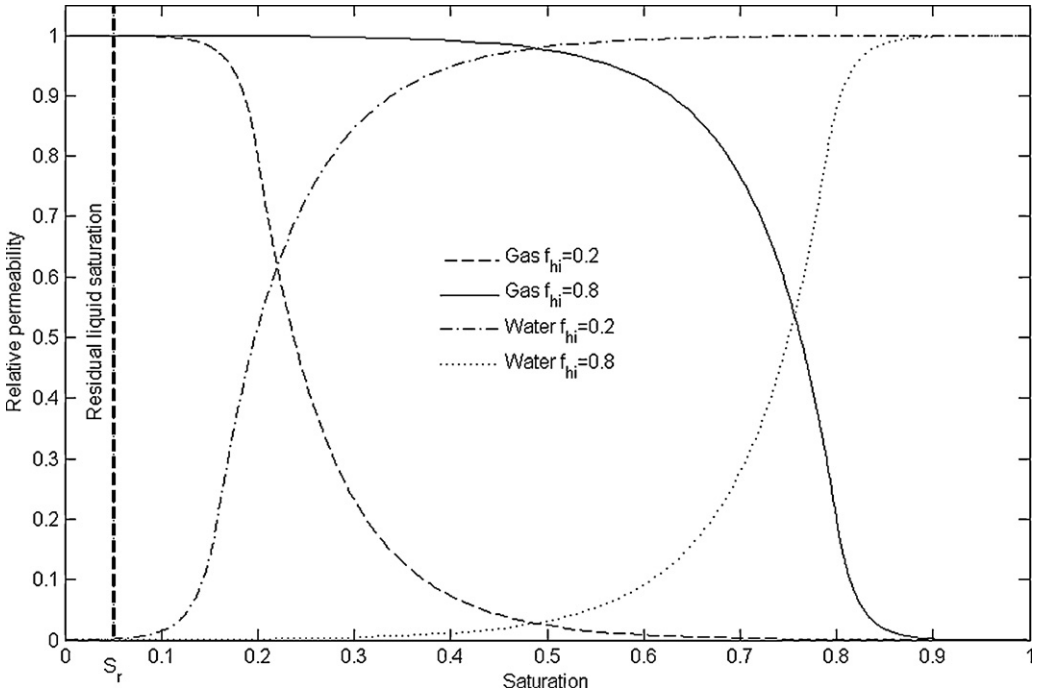

Fig. 6. Relative permeabilities of water and gas in the carbon paper GDL.

Fig. 3. As can be seen, the value of saturation increases greatly as the hydrophilic pore fraction f_{hi} increases from 0.2 to 0.8. This increase should correspond to more hydrophilic pores and larger porosity on lower PTFE loadings. At the same time, the value of capillary pressure increases as the hydrophilic pore fraction f_{hi} decreases, which means that capillary pressure increases with the addition of PTFE. This increase is caused by the decrease of the total pore space available for the water to occupy and the increase in the amount of hydrophobic pores.

In addition, from Fig. 3, it also can be seen that at a hydrophilic pore fraction lower than 0.5, i.e., for a nearly hydrophobic case, the capillary pressure increases slowly with increasing s at low liquid saturations but quickly when saturation is higher. It is due to that few hydrophilic capillaries exist and liquid water prefers to fill the large hydrophobic capillaries. While at a hydrophilic pore fraction higher than 0.5, i.e., for a nearly hydrophilic case, the opposite result is obtained because a lot of hydrophilic capillaries exist and the small hydrophilic capillaries are first to be filled.

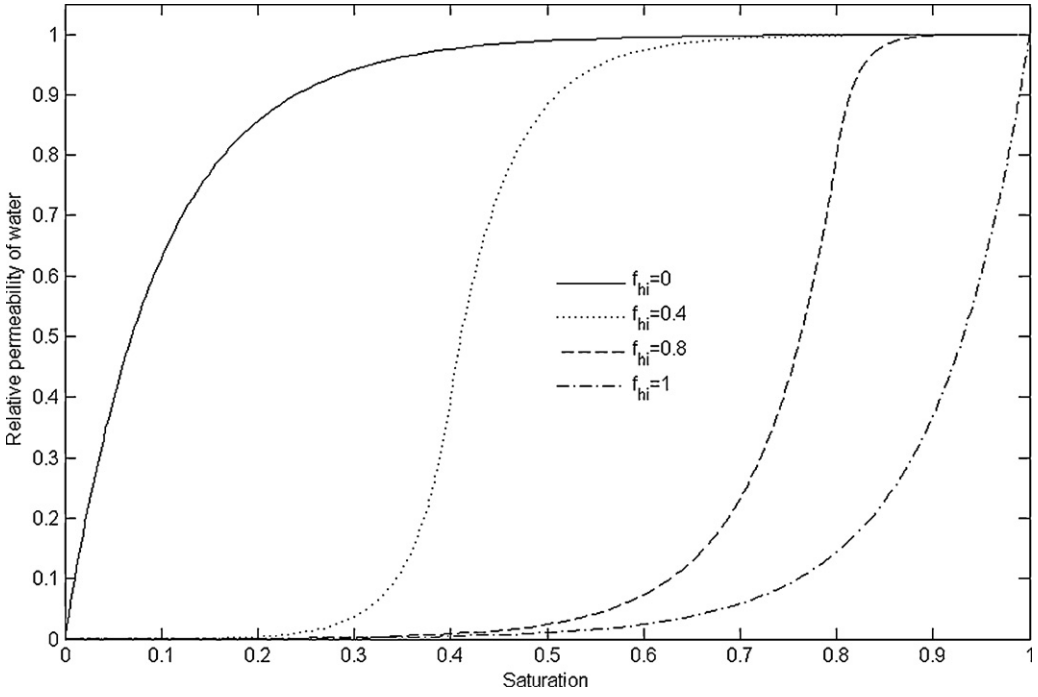

Fig. 7. Water relative permeabilities as function of water saturation for different hydrophilic pore fraction.

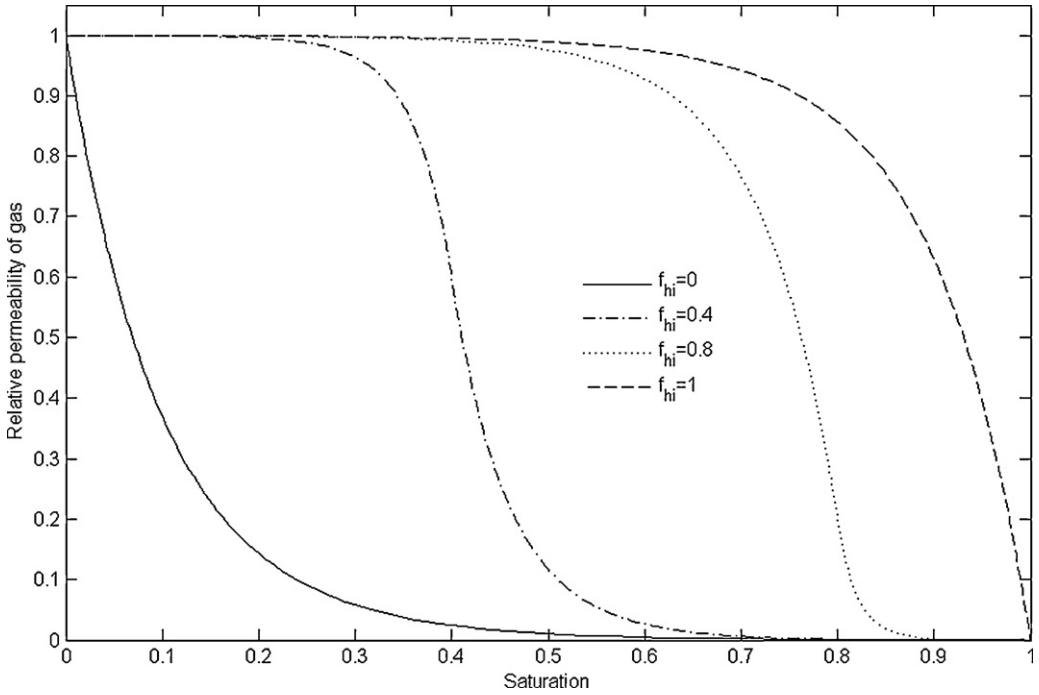

Fig. 8. Gas relative permeabilities as function of water saturation for different hydrophilic pore fraction.

Fig. 3 also shows that for the mixed wettability GDL the variation of p_c–s curve exhibits a trend of a slow increase at lower and higher capillary pressure but a fast raise around zero capillary pressure. The occupation of small hydrophilic capillaries at the beginning of condensation leads to the slow increase of p_c–s curve at negative capillary pressure. After this, the fast raise of p_c–s curve around zero capillary pressure is attributed to the liquid water filling in the large hydrophilic capillaries as well as the large hydrophobic capillaries. And then the slow increase of p_c–s curve at positive capillary pressure is contributed by the occupation of the rest small hydrophobic capillaries.

The effects of tortuosity and pore area fractal dimensions on p_c–s curve were investigated, as shown in Figs. 4 and 5, respectively. It can be seen that for a hydrophilic case the value of capillary pressure decreases with the increase of fractal dimensions at a given saturation and the value of saturation increases as the fractal dimensions increase at a given capillary pressure while for a hydrophobic case the opposite result is observed. From Eq. (1) and Eq. (4), we can know that a larger tortuosity and pore area fractal dimensions

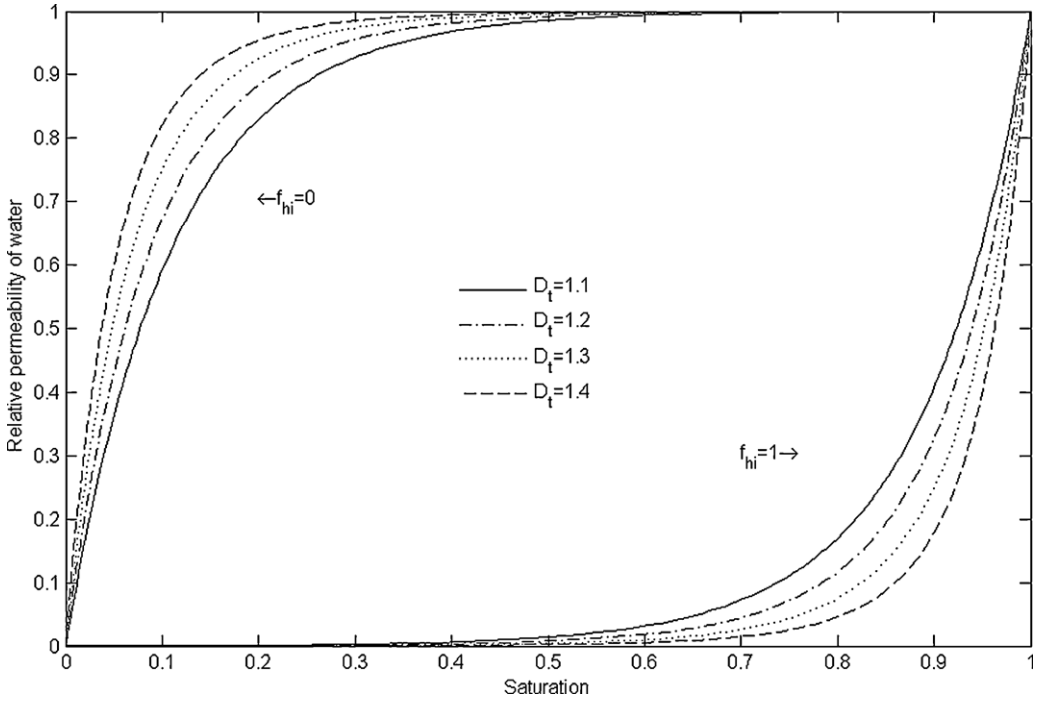

Fig. 9. Effect of tortuosity fractal dimension D_t on water relative permeability.

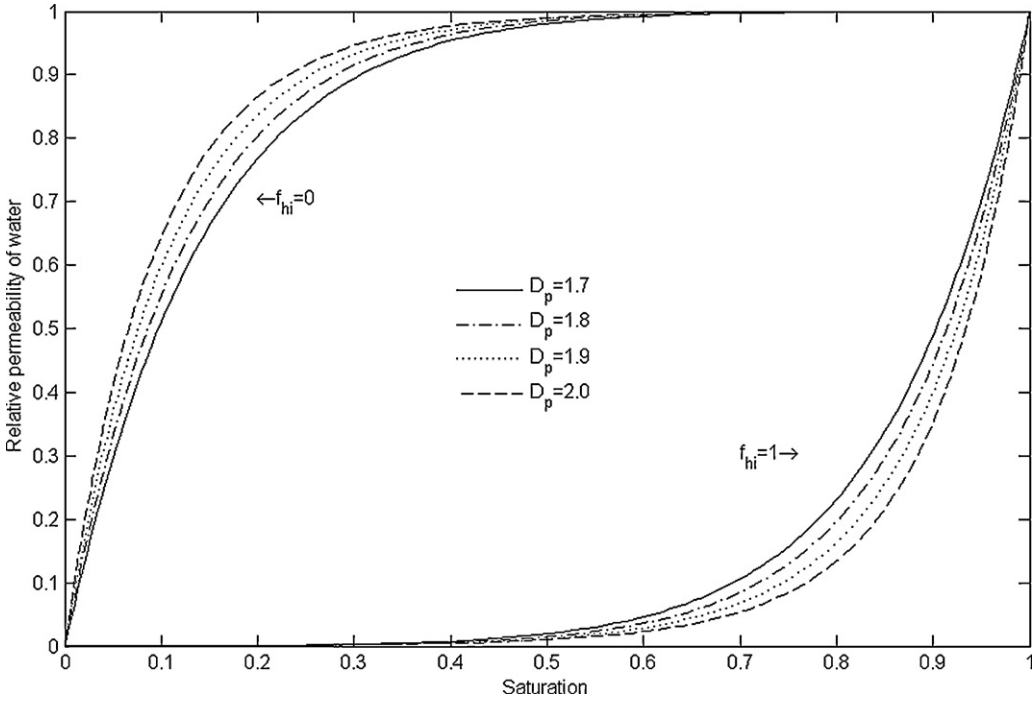

Fig. 10. Effect of pore area fractal dimension D_p on water relative permeability.

correspond to a longer capillary length and an increasing capillary number, respectively. The above results indicate that higher fractal dimensions result in greater increments of the number and length for smaller capillaries and a lower fraction of pore space contributed by the large capillaries. Therefore, for the hydrophilic GDL with higher fractal dimensions, more small capillaries will be occupied by liquid water at a given capillary pressure, leading to a higher saturation. While for the hydrophobic case, the opposite conclusion can be drawn, this is caused by the first occupation of large capillaries.

5.2. Predicted relative permeability

The fractal prediction on gas and water relative permeability for $f_{hi} = 0.2$ and 0.8 is presented in Fig. 6. It is seen that the relative permeability of the liquid phase is zero until liquid water saturation exceeds the threshold value at residual liquid saturation. Fig. 6 also shows that for the GDL of the mixed wettability, the behavior of water relative permeability versus saturation is controlled by three distinct regimes, i.e., a slow increase regime, a fast raise regime and again a slow increase regime, whereas that of gas relative permeability versus saturation is controlled by three other regimes, i.e., a slow decrease regimes, a fast drop regime and again a slow reduction regime. The explanation for this result is similar to that for the variation of p_c–s curve in the mixed-wettability case.

Figs. 7 and 8 show that the variations in relative permeability with the saturation for different hydrophilic pore fractions. The water relative permeability increases and the gas relative permeability decreases with the reduction of hydrophilic pore fraction. It is also seen that water relative permeability of the hydrophobic case is much larger than that of the hydrophilic case; while for gas relative permeability the opposite result is obtained. Therefore, for the goal to remove liquid water, a hydrophobic GDL is more suitable than the hydrophilic one for its high water relative permeability. While for the goal to maintain a certain quantity of water, a hydrophilic GDL is better for its low water relative permeability.

Figs. 9 and 10 show that the water relative permeability varies with the saturation for different values of tortuosity and pore area fractal dimensions, respectively. The results indicate that the water relative permeability of the hydrophilic case decreases and that of the hydrophobic case increases as the two fractal dimensions increase, which has been observed by the study of He et al. [24].

6. Conclusions

The purpose of this study is to propose theoretical models to determine the saturation, water and gas relative permeability of the GDL in PEMFCs. To this end, the relationships between the saturation, relative permeability and the microstructure of the GDL are considered using fractal methods, respectively. To validate the proposed fractal model of saturation versus capillary pressure, we compare it to experimental data and three empirical models that are widely used in the research of p_c–s curve. It can be concluded that in the case of mixed wettability, our fractal model is better for a good agreement with the experimental data, whereas these empirical models are not suitable for the GDL of mixed wettability due to obvious deviation between their results and the experimental data. After this, the effects of PTFE, tortuosity and pore area fractal dimensions on p_c–s curve are investigated. It is seen that the saturation is positively correlated with the two fractal dimensions for a hydrophilic case and the hydrophilic pore fraction, whereas it is negatively correlated with the two fractal dimensions for a hydrophobic case. And the capillary pressure is negatively correlated with the two fractal dimensions for a hydrophilic GDL and the hydrophilic pore fraction, whereas it is positively corrected with the two fractal dimensions for a hydrophobic GDL. These results indicate that higher fractal dimensions corresponds to greater increments of the number and length for smaller capillaries and a larger fraction of pore space contributed by the small capillaries. Furthermore, the prediction on gas and water relative permeability and the analysis on parametric effect are taken through the proposed models of water and gas relative permeability. Water relative permeability increases with the increases in the two fractal dimensions for the hydrophobic GDL and liquid water saturation, whereas it decreases with the increases in these fractal dimensions for the hydrophilic GDL and hydrophilic pore fraction at a given saturation.

As for gas phase, gas relative permeability is positively correlated with hydrophilic pore fraction, while it is negatively correlated with liquid water saturation.

The proposed models provide a bridge between microscale and macroscale models of PEMFCs. In future studies, we will leverage our previous work on the properties of the GDL to perform multi-scale and two-phase modeling of PEMFCs and thus facilitate the design of the GDL and of PEMFCs.

Acknowledgements

We would like to acknowledge the financial support of Project 51106116 supported by National Natural Science Foundation of China and of the Fundamental Research Funds for the Central Universities.

References

[1] J.D. Fairweather, P. Cheung, D.T. Shwartz, J. Power Sources 195 (2010) 787–793.
[2] Q. Ye, T.V. Nguyen, J. Electrochem. Soc. 154 (2007) B1242–B1251.
[3] C.S. Kong, D.-Y. Kim, H.-K. Lee, Y.-G. Shul, T.-H. Lee, J. Power Sources 108 (2002) 185–191.
[4] L.R. Jordan, A.K. Shukla, T. Behrsing, N.R. Avery, B.C. Muddle, M. Forsyth, J. Appl. Electrochem. 30 (2000) 641–646.
[5] E. Antolini, A. Pozio, L. Giorgi, E. Passalacqua, J. Mater. Sci. 33 (1998) 1837–1843.
[6] M.V. Williams, E. Begg, L. Bonville, H.R. Kunz, J.M. Fenton, J. Electrochem. Soc. 151 (2004) 1173–1180.
[7] J.T. Gostick, M.W. Fowler, M.A. Ioannidis, M.D. Pritzker, et al., J. Power Sources 156 (2006) 375–387.
[8] J.T. Gostick, M.A. Ioannidis, M.W. Fowler, M.D. Pritzker, Electrochem. Commun. 10 (2008) 1520–1523.
[9] D. Natarajan, T.V. Nguyen, J. Power Sources 115 (2003) 66–80.
[10] L. Pisani, G. Murgia, M. Valentini, B. D'Aguanno, J. Electrochem. Soc. 149 (2002) A898–A904.
[11] Z.H. Wang, C.Y. Wang, K.S. Chen, J. Power Sources 94 (2001) 40–50.
[12] R.L. Nava, R.H. Rauschenbach, M. Mangold, K. Sundmacher, Int. J. Hydrogen Energy 36 (2011) 1637–1653.
[13] H. Ju, J. Power Sources 185 (2008) 55–62.
[14] J.H. Nam, M. Kaviany, Int. J. Heat Mass Transfer 46 (2003) 4595–4611.
[15] Y. Wang, J. Power Sources 185 (2008) 261–271.
[16] E.C. Kumbur, K.V. Sharp, M.M. Mench, J. Electrochem. Soc. 154 (2007) B1295–B1304.
[17] N. Zamel, X.G. Li, Int. J. Energy Res. 32 (2008) 698–721.
[18] H. Wu, X.G. Li, P. Berg, Electrochim. Acta 54 (2009) 6913–6927.
[19] X. Wang, T.V. Nguyen, J. Electrochem. Soc. 155 (2008) B1085–B1092.
[20] N. Zamel, X.G. Li, J. Becker, A. Wiegmann, Int. J. Hydrogen Energy 36 (2011) 5466–5478.
[21] P.K. Sinha, C.-Y. Wang, Chem. Eng. Sci. 63 (2008) 1081–1091.
[22] A.Z. Weber, J. Newman, Chem. Rev. 104 (2004) 4679–4726.
[23] A.Z. Weber, R.M. Darling, J. Newman, J. Electrochem. Soc. 151 (2004) A1715–A1727.
[24] G.L. He, Z.C. Zhao, P.W. Ming, A. Abuliti, C.Y. Yin, J. Power Sources 163 (2007) 846–852.
[25] A.Z. Weber, J. Power Sources 195 (2010) 5292–5304.
[26] Y. Shi, J.S. Xiao, M. Pan, R.Z. Yuan, J. Wuhan Univ. Technol. Mater. Sci. Ed. 21 (2006) 22–25.
[27] R. Pitchumani, B. Ramakrishnan, Int. J. Heat Mass Transfer 42 (1999) 2219–2232.
[28] R. Wu, Q. Liao, X. Zhu, H. Wang, Int. J. Heat Mass Transfer 54 (2011) 4341–4348.
[29] A.Z. Weber, J. Newman, J. Electrochem. Soc. 151 (2004) A326–A339.
[30] D.E. Xue, H.X. Wang, C.S. Zhang, S.S. Xun, Permeation Physics in Porous Media, Petroleum Industry Publishing Company, Beijing, vol. 8, 1982, p. 43.
[31] J.D. Fairweather, P. Cheung, J. St-Pierre, D.T. Schwartz, Electrochem. Commun. 9 (2007) 2340–2345.
[32] P. Cheung, J.D. Fairweather, D.T. Schwartz, J. Power Sources 187 (2009) 487–492.
[33] Y. Shi, J.S. Xiao, M. Pan, R.Z. Yuan, J. Power Sources 160 (2006) 277–283.